Preparation and characterization of air nanofilters based on cellulose nanofibers

International Journal of Biological Macromolecules 182 (2021) 1392–1398

Contents lists available at ScienceDirect

International Journal of Biological Macromolecules

journal homepage: http://www.elsevier.com/locate/ijbiomac

Preparation and characterization of air nanofilters based on cellulose nanofibers

Sima Sepahvand [a,*], Mohsen Bahmani [b], Alireza Ashori [c,*], Hamidreza Pirayesh [a], Qingliang Yu [d], Mostafa Nikkhah Dafchahi [e]

[a] Department of Wood and Paper Science and Technology, Natural Resources Faculty, University of Tehran, Iran
[b] Department of Natural Resources and Earth Science, Shahrekord University, Shahrekord, Iran
[c] Department of Chemical Technologies, Iranian Research Organization for Science and Technology (IROST), Tehran, Iran
[d] Department of the Built Environment, Eindhoven University of Technology, P.O. Box 513, 5600 MB Eindhoven, the Netherlands
[e] Department of Wood and Paper Science and Technology, Natural Resources Faculty, University of Sari, Iran

ARTICLE INFO

Article history:
Received 4 April 2021
Received in revised form 11 May 2021
Accepted 12 May 2021
Available online 14 May 2021

Keywords:
Cellulose nanofiber
Air nanofilter
Chitosan
CO_2 adsorption
Particulate matter

ABSTRACT

One of the most important environmental issues in the world today is the problem of air pollution, which includes particulate matter (PM) and greenhouse gases (mainly CO_2). The production of efficient sustainable filters to overcome this concern as well as to provide an alternative to synthetic petroleum-based filters remains a demanding challenge. The purpose of this research was to first produce novel cellulose nanofibers (CNF) based nanofilter from a combination of CNF and chitosan (CS) and then evaluate its applicability for air purification. A number of structural and chemical properties as well as CO_2 and PM adsorption efficiency of the modified CNF, were determined using advanced characterization techniques. After pretests, we determined the optimum loading for the CS was 1 wt%, and upon producing the samples, the CNF loadings (1, 1.5, and 2 wt%) were chosen as one variable. For particle absorption, the PM sizes (0.1, 0.3, 0.5, and 2.5 μm) were kept as other variables. Based on SEM results, we concluded the higher the concentration of CNF the higher the specific surface area and the lower the porosity and the diameter of the pores, which was confirmed by the BET test. Furthermore, the results showed that increasing the concentration of modified CNFs increases the adsorption rate of CO_2 and PM and that the highest adsorption of CO_2 and PM belonged to the 2% modified CNF.

1. Introduction

Particulate matter (PM) is a significant environmental concern worldwide [1]. To be precise, PM is a complicated mixture of fine particles. Liquid droplets classified by size, i.e., $PM_{2.5}$ represents fine particles and liquid droplets less than 2.5 μm and $PM_{2.5\text{-}10}$ represents fine particles and liquid droplets less than 2.5–10 μm. The air in industrial and urban areas usually contains different combinations of pollutants, including PM of various sizes and chemical mixtures, and most importantly, particles less than 2.5 μm [2]. Polluted air includes various chemical and organic components, like carbon-derived species (CO_2 and CO), sulfur, and nitrogen-based inorganic compounds (SiO_2, SO_2^{2-}, SO_4^{2-}, and NO^{3-}) [3–6]. $PM_{2.5}$ is found in the atmosphere and is predominately produced from gas-to-particle conversion processes and combustion. $PM_{2.5}$ deposits in the human respiratory tract have been proven to be involved in lung diseases, heart diseases, and premature death [7]. Carbon dioxide (CO_2) is another dominant air pollutant, and it is generally believed that increased concentrations of atmospheric CO_2 are an important cause of global warming. In other words, as CO_2 is the most prevalent gas produced on earth, it has an immense impact on the environment, chiefly due to its toxicity. Capture, storage, and exploitation of emitted CO_2 are major challenges for environmentalists [8–10]. Traditionally, petroleum-based filters, such as polyethylene (PE), polypropylene (PP) and polyvinylidene fluoride (PVDF), are used to absorb PM. Generally, these filters are not biodegradable and cause different environmental pollution, usually needing hundreds of years to degrade naturally [1]. Therefore, the production of high-efficiency air filtering materials capable of simultaneously adsorbing PM less than 2.5 μm and CO_2 is in demand. Developing technologies combining different materials and process mechanisms are being proposed for CO_2 adsorption. Among these, the adsorption process based on alkanolamine—water solutions has been gaining a lot of attention. However, alkanol-amines are highly toxic, very corrosive, and energy-intensive [11]. Material that can efficiently adsorb CO_2 have certain specific traits, including high reactivity, large specific surface area, high selectivity, low basis weight, easy and low-cost technologies, environmentally friendly (sustainable), and in some cases, surface functionalization with amino groups is often necessary to improve their efficiency [12–14].

* Corresponding authors.
E-mail addresses: seppahvand.s@ut.ac.ir (S. Sepahvand), ashori@irost.ir (A. Ashori).

https://doi.org/10.1016/j.ijbiomac.2021.05.088
0141-8130/

Cellulose is the most abundant natural biopolymer compound and is customarily obtained from wood and agricultural residues. Wood, however, is the most commercial natural source of cellulose. Cellulose has unique characteristics, including being a nontoxic material, sustainability, renewability, recyclability, low density (1.6 g/cm^3), high aspect ratio, biodegradability, low cost, good mechanical properties, and high specific surface area (150 m^2/g) [15–17]. The cellulose surface consists mainly of hydroxyl groups (-OH functional groups) that can directly interact with modified polymers. Surface modification of cellulose with a modified polymer increases its functional properties and makes it more appropriate for a variety of applications [15]. Increasing the reactivity and content of cellulose surface hydroxyl groups so that they react with amine modification of nanocellulose is recommended [17]. It has been suggested that the surface of cellulose could be chemically modified for better CO_2 and PM adsorption by altering the reaction of a functional group from the organo-modified agents and OH on the cellulose surface. Derivative chitosan (CS) is usually obtained by partial deacetylation of *N*-acetyl groups from chitin (the second most abundant natural polysaccharide). CS is a linear copolymer made up of β1–4 linked *N*-acetylglucosamine (GLcAc) and glucosamine (GLcN) units whose high molecular structure is similar to cellulose and chitin [18]. CS has good biocompatibility and biodegradability, and all derivatives of CS possess good water absorbency and show antibacterial activities due to the existence of its amino groups, which makes them very practical [19,20]. Being similar in nature and chemical structure, the large amount of OH groups in the two polysaccharides and their availability as natural, cheap bio-polymers make them easily blended complementary bio-polymers. Moreover, due to its cationic property owing to the presence of the first type of amine group (derived from the polymer body of CS) and also the polyelectrolyte's ability to absorb negatively on negatively charged surfaces in acidic media, CS can be used in different biomaterials because CS with its cation-charged amine group reacts with anionically charged hydroxyl groups [21,22].

Several studies have been conducted on nanofibers' pollution filtration efficiency. Liu et al. [23] developed a clear filter for air purification using electrospun nanofibers with various petrochemical based polymers. They concluded that fiber diameter and surface chemistry are very effective in absorbing air pollutants. They proposed that among the common synthetic polymers, polyacrylonitrile can adsorb more particles due to its bipolar groups and its adsorption efficiency is about 95–100% in 100 h [23]. Desai et al. examined filters made of nanofibers and CS and evaluated their usability for air filtration. The nanofibers were electrospun on a nonwoven polypropylene substrate using chitosan/polyethylene oxide (PEO) mixtures and revealed that the filtration efficiency of the formed nanofiber substrate was strongly related to the fiber size and the amount of chitosan [24]. Valdibenito et al. (2018) studied a film of cellulose nanofibers modified with -N3-[(trimethoxycyl) propyl] ethylenediamine to adsorb CO_2 and reported that after exposing the modified cellulose nanofiber films to CO_2 for 3 h the CO_2 uptake concentration increased at 25 °C [25].

In this study, an emulsion freeze-drying technique was used to produce nanofilters for air purification. This method was chosen because it is a simple method in which factors such as dispersed phase volume fraction, polymer concentration, molecular weight, and ice crystal growth during the process effect the porosity and pore size of samples [26]. To reach our goal, the surface of a cellulose nanofiber (CNF) was functionalized using chitosan (CS), poly [β-(1, 4)-2amino-2-deoxy-D-glucose], using a direct, convenient method without the use of any hazardous solvent. CS was chosen as the surface modifier because of its unique features, including good antibacterial and antifungal properties, low toxicity, biocompatibility, simplistic structure, biodegradability, high reactivity, sustainability, minimal cost, and amino groups. Hence, this study was conducted to produce first CS-grafted CNF nanofilters. The nanofilters were then characterized by scanning electron microscopy (SEM) and attenuated total reflectance-Fourier transform infrared spectroscopy (ATR-FTIR). Then, the novel filters were compared with pristine CNF material. Lastly, the results of the characterization and the adsorption rate of the proposed air purification nanofilters are reported.

2. Materials and methods

2.1. Materials

2.1.1. CNF preparation

Birch kraft pulp was obtained from SCA Munksund AB (Piteå, Sweden). An ultrafine friction grinder MKZA10-20J (Masuko Sangyo Co., Japan) was used to grind the pulp at 2.2 wt% consistency during the CNF fibrillation process. Before the grinding process, the suspension was dispersed employing a shear mixer (Silverson L4RT Silverson Machine Ltd., England). After feeding the suspension into the grinder, the grinding stones were set in contact mode and adjusted until they reached 90 μm (negative). Coarse silicon carbide (SiC) stones were used with a rotor speed of 1500 rpm. The grinding was complete when a maximum viscosity gel was obtained [17].

Transmission electron microscopy (TEM), FEI Tecnai 20 Sphera, was used to study the CNF distribution and diameter. The TEM image of the isolated CNF showed a width ranging from 20 to 50 nm, indicating the CNF used was below 100 nm.

CS powder (M_w 400 kDa) and DA 99.5% (purchased from Sigma Aldrich, USA) was used for the modifications. Acetic acid (99.5%, purity) was bought from Sigma Aldrich (USA). All solutions were prepared using distilled water (Fig. 1).

2.1.2. Production of the air nanofilters

The CNF suspensions (1, 1.5 and 2 wt%) were placed on a stirrer adjusted at 480 rpm for 3 h at room temperature. The CS powder (1 wt%, based on the results of the pretests) was dissolved in an acetic acid/water solution (1/99 (v/v)) and stirred at 60 °C for 2 h. Then, CS was added to the CNF suspension with a volume of 15 cm^3 at room temperature and stirred for additional 8 h using a magnetic stirrer. The pH of the solution was acidic and the CNF-CS suspension was centrifuged at 5000 rpm for 5 min to remove the excess CS that had grafted onto the CNF. Finally, the CNF-CS suspension was placed inside a 3 cm diameter Teflon polytetrafluoroethylene (PTFE) and fixed on the surface of a 4 cm diameter copper cylinder so that the bottom 4 cm of the cylinder was placed in liquid nitrogen (−196 °C), then the prepared mixtures were filled into the Teflon tube. The mixtures were frozen from the bottom to the top of the container. Then, samples were dried in a freeze dryer (Alpha 1–4 LD plus from Christ) at a sublimating temperature of −53 °C at a pressure of 0.073 mbar for 72 h. Finally, all samples were conditioned at 23 °C and 50% relative humidity for one day. The resulting materials are referred to as CS-CNF.

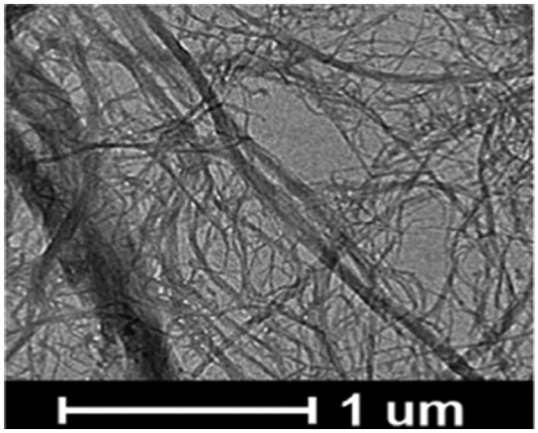

Fig. 1. A typical TEM image of CNF.

2.2. Characterization of the air nanofilters

2.2.1. Attenuated total reflectance-Fourier transforms infrared spectroscopy (ATR-FTIR)

ATR-FTIR is a technique used to evaluate the structural variations of samples. The structural changes of the air nanofilters, unmodified and modified CNF, were recorded using the attenuated total reflection (ATR) method (Gladi ATR) of ATR-FTIR spectrometry with a Perkin Elmer Frontier TM Spectrometer (spectrum 400 FT-IR) in a spectral range from 400 to 4000 cm^{-1} and a scanning resolution of 4 cm^{-1} (16 scans for each sample).

2.2.2. Scanning electron microscopy (SEM)

The surface morphology of the air nanofilters, the unmodified and modified CNF, was examined by SEM. The SEM observations were carried out using a Phenom ProX (Netherlands) operated at an accelerating voltage of 10 kV. All samples were sputtered-coated (30 s and 65 mA) with a gold layer of approximately 15 nm thickness. Also, the presence of amine groups (NH_2) on the surface of the CNF was detected using an energy dispersive x-ray spectroscopy (EDX).

2.2.3. Assessment of density and porosity

The density of the air nanofilters was determined based on the ratios of its weight to volume. The mass of the air nanofilters was measured using an analytical balance (readability 0.0001 g, Analytical Balance, Metter Toledo), and the dimensions (diameter and height) of the air nanofilter were measured using a digital calliper. The porosity (P) of the air nanofilters was calculated based on the mass density of the nanofilter (ρm) and the somatogenic density (ρs = 1.520 g/cm^3) of CNF by Eq. (1).

$$P(\%) = \left(1 - \frac{\rho_m}{\rho_s}\right) \times 100 \quad (1)$$

2.2.4. Brunauer-Emmett-Teller (BET) analysis and pore size distribution

The Brunauer-Emmett-Teller specific surface area (BET) was determined by N2 physisorption using a micrometrics TriStar II automated system. About 0.1–0.2 g of the air nanofilter samples were first dried in the micrometrics TriStar II at 115 °C for 4 h and then degassed in the micrometrics TriStar II at 115 °C for 18 h prior to the analysis and followed by N2 adsorption at 196 °C. BET analysis was carried out for a relative vapor pressure (P/P0) of 0–1 at −196 °C. The average pore size of the CNF air nanofilter was estimated from the nitrogen desorption isotherm according to the analysis of Barrett-Joyner-Halender [17,27].

2.2.5. CO_2 adsorption measurements

Pressurized air, including 500 ppm CO_2 concentration, was used to evaluate the CO_2 adsorption capacity of the synthesized air nanofilters. All the CO_2 adsorption experiments were carried out at an air flow rate of 0.8 L/min, 1 bar pressure, at room temperature, and 30% relative humidity for 8 h. The CO_2 adsorption efficiency (η) was experimentally determined from the inlet and outlet CO_2 concentration. A steady state was achieved according to the expression given by Eq. (2) [17,28].

$$\eta = \left(1 - \frac{C_{CO_2 out}}{C_{CO_2 in}}\right) \times 100 \quad (2)$$

where, C_{co_2in} and C_{co_2out} are the inlet and outlet CO_2 concentration, respectively.

2.2.6. Adsorption test of PM by air nanofilters

The removal efficiency (E %) was explored under the environmental conditions described above, with 10 L/min airflow rate for 8 h, and the calculation was done using Eq. (3) [2].

$$E(\%) = \left(\frac{C_u - C_d}{C_u}\right) \times 100 \quad (3)$$

where, C_u and C_d are the concentration of PM before and after adsorption by the air nanofilters, respectively.

2.2.7. Quality factor (QF) measurement of the nanofilters

The overall performance of porous air nanofilters, representing both efficiency and pressure drop, is defined by QF. In other words, QF is an important factor to assess the quality of air nanofilters. The QF was calculated based on Eq. (4) [29].

$$QF = -Ln(1 - E\%)/\Delta P \quad (4)$$

where, E is the PM removal efficiency and ΔPis the pressure drop of air nanofilters.

2.3. Statistical analysis

SPSS (Version 20.0) Analysis of Variance (ANOVA) was used to examine the obtained data and followed by Duncan's Multiple Range Test with a confidence level of 95% to determine if there was any difference between the means.

3. Results and discussion

3.1. ATR-FTIR

The infrared spectrum related to the CNF was taken before and after modification to determine the chemical structure and also to confirm the amino chitosan groups' bond on the CNF. The spectroscopic results are shown in Fig. 2. Signals related to the tensile vibration of OH in the CNF spectrum appeared in the range of 3600–3000 cm^{-1} (3335 cm) [30]. Peaks in the range of 3000–2800 cm^{-1} correspond to the tensile vibration of C—H and CH_2 bands in CNF groups before and after the modification [31]. All the peaks were identified as typical cellulose peaks. In this study, the peaks around 1314 and 1430 cm^{-1} in both the unmodified and modified CNF spectra could be assigned to the symmetric bending of CH_2 and the bending vibrations of the C—H and C—O groups of the rings in polysaccharides, respectively. Furthermore, the absorbance peaks in the range 1162–1030 cm^{-1} are attributed to C—O stretching and C—H rocking vibrations of the pyranose ring skeleton and the bands in the range 1000–1200 cm^{-1} are assigned to the carbohydrate rings of the cellulose skeleton [15,32]. The vibration peak at 900–895 cm^{-1} in the spectra which are symmetric in polysaccharides is usually assigned to the glycoside bonds, represents the β-glucosidic linkage between glucose units in cellulose [15,33,34]. After modifying CNF with CS, a new peak appeared around 1548 cm^{-1}. This new peak was related to the bending vibration of NH_2 groups, which

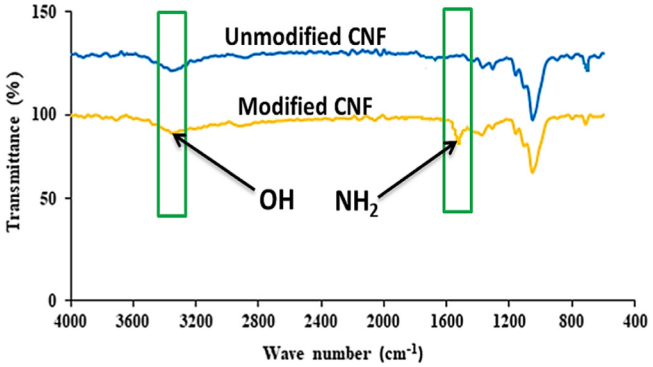

Fig. 2. ATR-FTIR spectra of unmodified and modified CNF (CNF-CS (1.5:1)) air nanofilters.

implied the presence of functional groups on the CNF surface, revealing that the CS has been successfully transplanted onto the CNF surface [30].

3.2. SEM and EDX

The morphological characteristics of unmodified and modified CNF air nanofilters are presented in Fig. 3A (a, b, c, and d). As can be seen, all the samples have a very porous structure and also contain an integrated cellulose network, which shows that the CNF are autonomously bonded together through a hydrogen bond to create a three-dimensional network. Fig. 3(a) shows the modified CNF surface has a reasonably porous matrix with relatively good dispersion. In addition, it has a large pore diameter and a more open and porous structure [35,36]. Fig. 3(b, c, and d) shows a more uniform surface developed on the CNF surface after modification with CS, which indicates the presence of CS on the surface fibers. Air nanofilters get stronger and more compact as the concentration of CNF increases, which represents a higher volume of CNF fibrils. In general, the dense structure resulted in an increase in specific surface area and a decrease in size porosity of the pores so that highest specific surface areas were related to the shape of Fig. 3d, c, and b respectively. An EDX attached to the SEM was used for elemental analysis of the modified CNF. Fig. 4(B) shows the modified CNF's EDX spectrum. The CNF modified with CS contains elements like carbon (C), oxygen (O), and nitrogen (N). Among these, C and O are the main components of CNF, while N is attributed to CS. Thus, the presence of CS on CNF was verified by EDX analysis [15].

3.3. BET, density, and porosity characteristics

Fig. 4(a, b, c, and d) represents the density, porosity, specific surface area, and pore diameters of both unmodified and modified air nanofilters. The density and specific surface area increased when the concentration of CNF increased (Fig. 4(a, c)), but the porosity and pore diameters decreased. However, the decrease in porosity and pore diameter can be seen in Fig. 4(d and d). So, concentration is a factor that affects the porosity, pore diameters, and density. Increasing the concentration leads to a denser and more compact structure, and consequently, a lower porosity and smaller pore diameters [17,30]. The results of the analysis of variance of samples were statistically significant with a 95% confidence level and the highest density and specific surface area, as well as the lowest porosity and pore diameter, were related to the CNF modified with a 2% concentration. In general, with increasing the concentration of modified CNF the specific surface area increased due to the increase in density as well as the presence of CS [15,28]. Also, as it can be seen, with the increasing concentration of modified CNF, the porosity and average pore diameter decreased, which can probably attributed to the increasing of density, which causes the air nanofibers to compress and become denser.

3.4. CO_2 adsorption

CNF aerogels are potentially good for use in air nanofilters, especially for CO_2 adsorption, due to their highly porous structure, low pore diameter, and high specific surface area [17]. The results obtained from the analysis of variance of the effect of different concentrations of modified CNF on the adsorption rate and output concentration of CO_2 compared with pure CNF indicated that with increasing concentration, adsorption amounts and CO_2 output concentrations were significantly (at 95% confidence level) changed (Table 1). Duncan's test also divided the adsorption values and the output concentration of CO_2 obtained in different concentrations used into three and four separate groups, respectively (Table 2) so that based on the obtained results, the use of 2% modified CNF led to the maximum amount of adsorption (4.8 mmol/g) as well as the minimum CO_2 outlet concentration (346.5 ppm). Fig. 5 (a) shows the concentration of CO_2 emissions from CNF aerogels at different concentrations of CNF. The higher the concentration of CNF, the lower the concentration of CO_2 output in comparison with the control sample. As Fig. 5(b) shows the capacity of adsorption for the unmodified CNF is 2.2 $mmol \cdot g^{-1}$, that is probably due to the formation of a tremendous surface OH group leading to the CO_2 adsorption. However, compared to the control sample, when the surface of CNF is modified by CS 1 wt% as well as increasing the concentration of CNF, the adsorption of CO_2 improved. This was reflected by the increasing adsorption capacity ranging from 2.6, 3.5, and 4.8 $mmol \cdot g^{-1}$ corresponding to the concentration of CNF 1, 1.5, and 2%, respectively. In fact, the adsorption of CO_2 for CS-modified CNF improved with increasing in the concentration of CNF so that the best result was related to the 2% modified CNF (4.8 $mmol \cdot g^{-1}$). Increasing the concentration of CNF led to an increase in the specific surface area and a reduction in pore diameter, which resulted in greater CO_2 adsorption. In addition, high concentrations of CNF are likely to increase the number of OH groups on the CNF surface, so more amino groups could react with surface OH groups by modifying the surface, which all contribute to higher CO_2 adsorption [17].

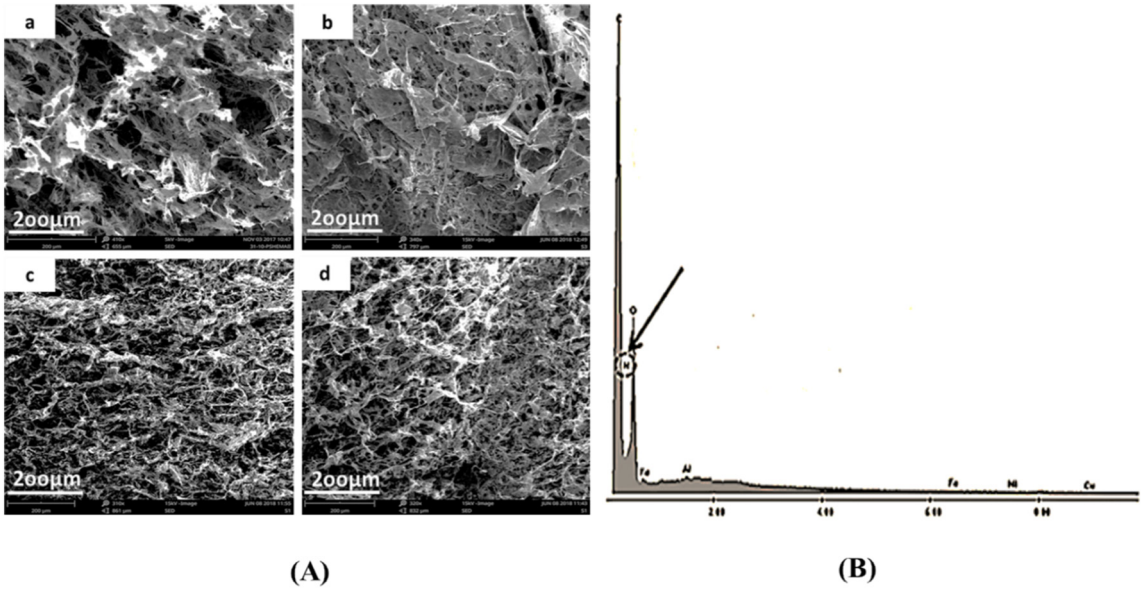

Fig. 3. (A) SEM images of (a) unmodified CNF, (b) modified CNF (1 wt%), (c) modified CNF (1.5 wt%), and (d) CNF (2 wt%) and (B) EDX spectrum of modified CNF (CNF-CS (1.5:1)).

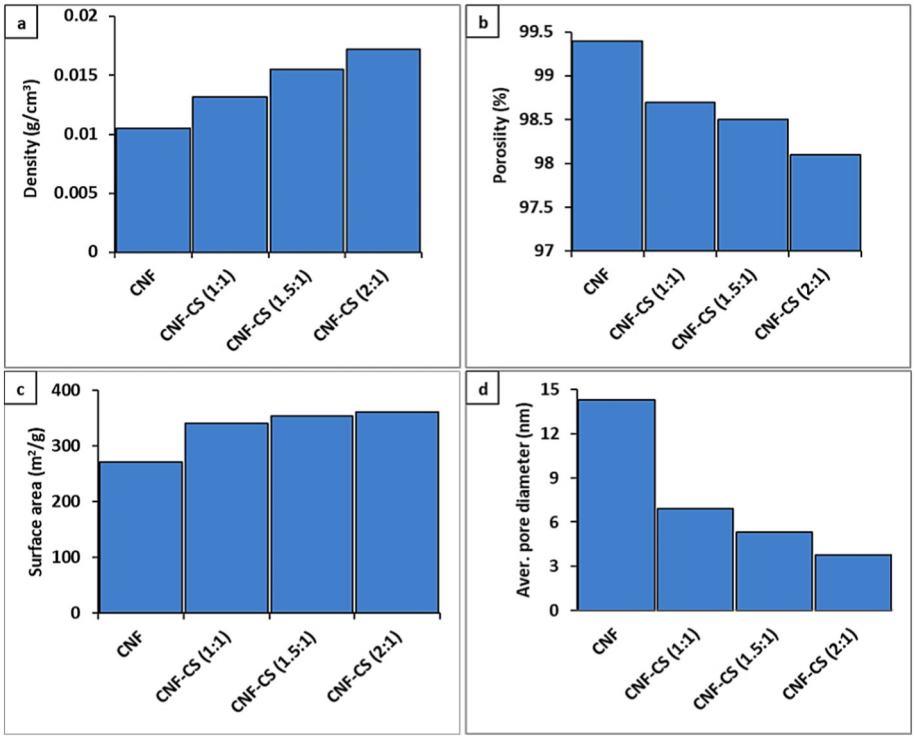

Fig. 4. (a) Density, (b) porosity, (c) surface area, and (d) average pores diameter the unmodified and modified CNF air nanofilters.

Table 1
Results of ANOVA the effect of CNF concentration on the adsorption rate and outlet CO_2 concentration.

Variable	Properties	S.O.V	SS	DF	MS	F	p
Concentration of CNF	CO_2 adsorption	Treatment	396.2803	3	17.1582	7.18	0.033
		Error	28.318	8	1.0553		
		Total	424.5983	11			
Concentration of CNF	CO_2 outlet concentration	Treatment	93.3878	3	11.2042	11.08	0.0264
		Error	54.2064	8	1.018		
		Total	147.5942	11			

SS, sum of squares; DF, degrees of freedom; MS, mean squares; F, F ratio; p, p value.

3.5. PM adsorption

Table 3 shows the results of analysis of variance of the effect of modified CNF concentration on the adsorption rate of different PM compared with unmodified counterparts. As can be seen, the concentration of CNF has led to a significant difference (statistical confidence level of 95%) of particle adsorption efficiency in different sizes of 0.5–1.5 μm. Also, in Table 4, Duncan test has placed the obtained adsorption efficiency values in four, three, and four different groups for particles with sizes of 0.1, 0.3, 0.5, and 2.5 μm, respectively. The highest adsorption efficiency was obtained for particles with a size of 2.5 μm and using 2% of modified CNF, which was 99.56%. In general, based on the obtained results, with increasing the concentration of CNF, a significant difference in the rate of adsorption efficiency in different sizes is observed.

Table 2
Duncan grouping the effect of CNF concentration on the adsorption rate and outlet CO_2 concentration.

Treatments/variables/properties	Outlet CO_2concentration	CO_2 adsorption
CNF	431^a	2.2^c
CNF-CS (1:1)	407.5^b	2.6^c
CNF-CS (1.5:1)	373.5^c	3.5^b
CNF-CS (2:1)	346.5^d	4.8^a

Different lowercase letters in the same column show the significant difference ($P < 0.05$).

Fig. 6 shows that increasing the concentration of modified cellulose nanofibers (1 to 2%) and the size of PM (0.1 to 2.5 μm) increases the adsorption efficiency of PM. The highest adsorption (99.56%) was related to the nanofilters with a 2% concentration and 2.5 μm PM. This increase in adsorption efficiency and performance of the resulting nanofilters could be due to two reasons. The first reason is the reduction of the pore diameter and increase of the specific surface area of the resulting nanofilters because a higher concentration increases the density and compaction of the CNF, which leads to an increase in specific surface area and a decrease in pore diameter [17,35]. Secondly, since the size of the PM is 2.5 μm larger than the pore diameter of the resulting nanofilters, these particles are not able to pass through the diameter of the resulting nanofilters, and consequently, the adsorption rate increased. Also, with regards to the adsorption of PM, the efficiency of nanofilters made of unmodified CNF was less than 0.1 μm (72.43%), which was lower (92.52%) than nanofilters made of the modified CNF. A surface modified by CS causes some particles less than 0.1 μm, including CO_2, CO, and CH_2O, to react chemically with the surface increasing the adsorption efficiency and performance of resulting filters. In general, nanofilters made from the modified CNF have a higher adsorption power, at 2.5 μm particles, than polyamide nanofilters (PI) and high-efficiency particulate air (HEPA) filters [31].

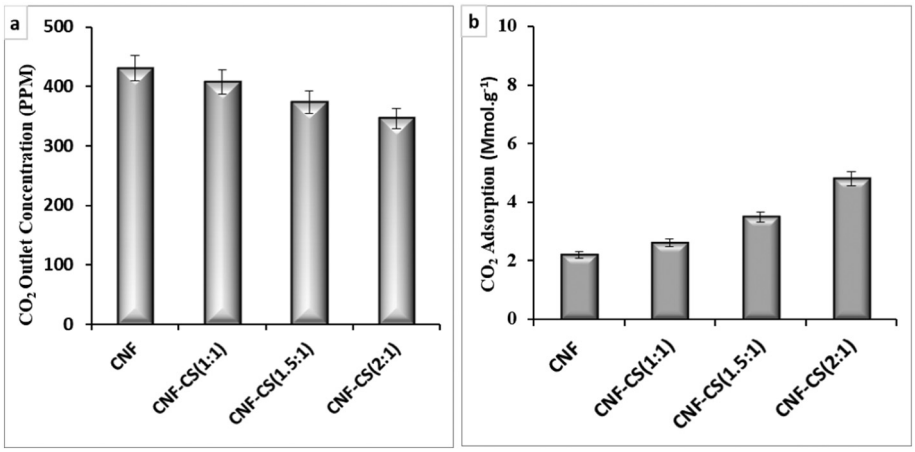

Fig. 5. (a) Outlet CO_2 concentration and (b) CO_2 adsorption of the unmodified and modified CNF nanofilters.

Table 3
Results of ANOVA the effect of CNF concentration on the adsorption rate of different PM.

Variable	Properties	S.O.V	SS	DF	MS	F	p
Concentration of CNF	$PM_{0.1}$ (μm)	Treatment	331.2013	3	41.563	27.49	0.0185
		Error	26.0072	8	2.1507		
		Total	357.2085	11			
Concentration of CNF	$PM_{0.3}$ (μm)	Treatment	308.5066	3	47.1064	18.75	0.0407
		Error	42.8916	8	2.873		
		Total	351.398	11			
Concentration of CNF	$PM_{0.5}$ (μm)	Treatment	448.2769	3	40.6027	11.75	0.0393
		Error	40.1963	8	1.996		
		Total	488.4732	11			
Concentration of CNF	$PM_{2.5}$ (μm)	Treatment	405.9793	3	42.8859	6.59	0.028
		Error	39.6641	8	2.0015		
		Total	445.6434	11			

SS, sum of squares; DF, degrees of freedom; MS, mean squares; F, F ratio; P, p value.

Table 4
Duncan grouping the effect of CNF concentration on the adsorption rate of different PM.

Treatments/variables/properties	The size of particulate matter (PM)			
	0.1 (μm)	0.3 (μm)	0.5 (μm)	2.5 (μm)
CNF	72.43^{d}	85.67^{c}	87.26^{c}	89.43^{c}
CNF-CS (1:1)	83.80^{c}	92.69^{b}	94.39^{ab}	95.72^{b}
CNF-CS (1.5:1)	88.45^{b}	94.87^{ab}	96.56^{a}	$97.93a^{b}$
CNF-CS (2:1)	92.52^{a}	96.88^{a}	97.77^{a}	99.56^{a}

Different lowercase letters in the same column show the significant difference ($P < 0.05$).

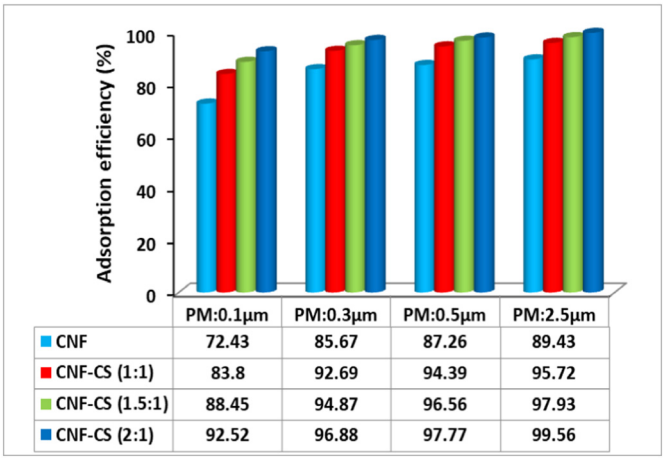

Fig. 6. PM adsorption of unmodified and modified CNF air nanofilters.

3.6. Pressure drop (ΔP) and quality factor (QF)

Two important factors affecting the performance of air nanofilters are pressure drop (Δ*P*) or airflow permeability and high removal efficiency. On the one hand, the performance of nanofilters is related to energy consumption, and the higher theΔ*P*, the higher the energy consumption. On the other hand, the overall performance of air nanofilters, considering both removal efficiency andΔ*P*, can be defined by a quality factor (QF) [3,29]. High filtration efficiency shows Δ*P* of less than 325 Pa at a standard air face velocity of 5 cm/s [17].

Table 5 shows a quantitative study of the effects of ΔP and QF on the unmodified and CS modified CNF. As can be seen, all air nanofilters made of CNF have a lower ΔP than the standard DOE, while the HEPA filter has a higher ΔP than the standard. A HEPA filter is 30 mm thick, which creates more empty spaces between the fibers resulting in more ΔP [29], while nanofilters made of CNF have a thickness of 1.2 mm, and the space between the fibers is fairly small. Moreover, as the concentration of modified CNF increases, the ΔP of the resulting nanofilters decreases. So, the lowest ΔP (79 Pa) and the highest QF (0.1021 Pa^{-1}) were related to the modified CNF with a concentration of 2%. This reduction might be related to its surface area, small pore diameter, pore volume, and pore structure [37].

4. Conclusions

In this study, a simple method was used to modify the surface of CNF using CS for better CO_2 and PM adsorption. Structural and chemical analyses as well as CO_2 and PM adsorption of the modified CNF were measured using advanced characterization techniques. Morphological study of CNF air nanofilters by SEM showed that the porosity and pore diameter of CNF air nanofilters decreased when the concentration of CNF increased, however, the specific surface area and density also increased so that no change in the structure as well as fiber dimensions was observed. The data of the BET test confirmed the results of the SEM images. Furthermore, the FTIR-ATR analysis revealed a new peak, NH_2, which proved that CS was grafted on the CNF surface. The results of CO_2 and PM adsorption showed that the highest adsorption belongs

Table 5
ΔP and QF in the air nanofilters made of unmodified and modified CNF.

Parameters	HEPA	CNF	CNF-CS (1:1)	CNF-CS (1.5:1)	CNF-CS (2:1)
ΔP (Pa)	425^{a}	241^{bc}	148^{b}	118^{c}	79^{d}
QF (Pa^{-1})	0.0058^{a}	0.0162^{a}	$0.0308b^{bc}$	0.0894^{b}	0.1021^{c}

Different lowercase letters in the same row show the significant difference ($P < 0.05$).

to the 2% modified CNF. In addition, PM adsorption results revealed that the unmodified and modified CNF air nanofilters were able to absorb particles less than 0.1 μm. Moreover, the adsorption efficiency increased when the PM sizes and concentration of CNF increased so that the highest adsorption rate (99.56%) of particles was related to 2% modified CNF air nanofilters and $PM_{2.5}$, which could be attributed to the high specific surface area, the small diameter of the pores through which the particles could not pass, and more functional groups on the air nanofilters surface. The air nanofilters made of unmodified and modified CNF had the lowest ΔP and the highest QF in comparison to HEPA filters. This could be due to the high specific surface, large pores volume, diameter of the pores, smaller thickness. In conclusion, using this method, modifications were able to tailor CNF surface properties without monotonous and unpractical solvent-exchange protocols to make effective sustainable air nanofilters.

Acknowledgments

The authors wish to thank the Eindhoven University of Technology (TU/e) for providing the necessary laboratory facilities for this work. In addition, many thanks goes for the University of Tehran and Iran Nanotechnology Initiative Council (INIC) for providing financial support during this research.

References

[1] X. Liu, H. Souzandeh, Y. Zheng, Y. Xie, W.H. Zhong, C. Wang, Compos. Sci. Technol. 138 (2017) 124–133.
[2] H. Souzandeh, B. Molki, M. Zheng, H. Beyenal, L. Scudiero, Y. Wang, W. Zhong, ACS Appl. Mater. Interfaces 9 (2017) 22846–22855.
[3] X. Han, L.P. Naeher, Environ. Int. 32 (2006) 106–120.
[4] H. Souzandeh, K.S. Johnson, Y. Wang, K. Bhamidipaty, W.H. Zhong, ACS Appl. Mater. Interfaces 8 (2016) 20023–20031.
[5] H. Souzandeh, L. Scudiero, Y. Wang, W.H. Zhong, Chem. Eng. 5 (2017) 6209–6217.
[6] R. Zhang, J. Jing, J. Tao, S.C. Hsu, G. Wang, J. Cao, C.S.L. Lee, L. Zhu, Z. Chen, Y. Zhao, Atmos. Chem. Phys. 13 (14) (2013) 7053–7074.
[7] D.Y. Pui, S.C. Chen, Z. Zuo, Particuology 13 (2014) 1–26.
[8] L.A. Darunte, K.S. Walton, D.S. Sholl, C.W. Jones, Chem. Eng. 12 (2016) 82–90.
[9] C. Knöfel, C. Martin, V. Hornebecq, P.L. Llewellyn, J. Phys. Chem. C 113 (2009) 21726–21734.
[10] D.Y. Leung, G. Caramanna, M.M. Maroto-Valer, Renew. Sust. Energ. Rev. 39 (2014) 426–443.
[11] F. Valdebenito, R. García, K. Cruces, G. Ciudad, G. Chinga-Carrasco, Y. Habibi, ACS Sustain. Chem. Eng. 6 (2018) 12603–12612.
[12] P. Bollini, S.A. Didas, C.W. Jones, J. Mater. Chem. 21 (39) (2011) 15100–15120.
[13] D.M. D'Alessandro, B. Smit, J.R. Long, Angew. Chem. Int. Ed. 49 (2010) 6058–6082.
[14] S. Sung, M.P. Suh, J. Mater. Chem. A 2 (2014) 13245–13249.
[15] H. Khanjanzadeh, R. Behrooz, N. Bahramifar, W. Gindl-Altmutter, M. Bacher, M. Edler, T. Griesser, Int. J. Biol. Macromol. 106 (2018) 1288–1296.
[16] N. Lavoine, I. Desloges, A. Dufresne, J. Bras, Carbohydr. Polym. 90 (2012) 735–764.
[17] S. Sepahvand, M. Jonoobi, A. Ashori, F. Gauvin, H.J.H. Brouwers, K. Oksman, Q. Yu, Carbohydr. Polym. 230 (2020), 115571, .
[18] B. Cheng, B. Pei, Z. Wang, Q. Hu, RSC Adv. 7 (2017) 42036–42046.
[19] A. Anitha, S. Sowmya, P.S. Kumar, S. Deepthi, K.P. Chennazhi, H. Ehrlich, R. Tsurkan, R. Jayakumar, Prog. Polym. Sci. 39 (2014) 1644–1667.
[20] S. Elkholy, K.D. Khalil, M.Z. Elsabee, M. Eweis, J. Appl. Polym. Sci. 103 (2007) 1651–1663.
[21] A. Bernkop-Schnürch, S. Dünnhaupt, Eur. J. Pharm. Biopharm. 81 (2012) 463–469.
[22] H. Vaghari, H. Jafarizadeh-Malmiri, A. Berenjian, N. Anarjan, Sustain. Chem. Process 1 (1) (2013) 1–12.
[23] C. Liu, P.C. Hsu, H.W. Lee, M. Ye, G. Zheng, N. Liu, W. Li, Y. Cui, Nat. Commun. 6 (2015) 1–9.
[24] K. Desai, K. Kit, J. Li, P.M. Davidson, S. Zivanovic, H. Meyer, Polymer 50 (15) (2009) 3661–3669.
[25] F. Valdebenito, R. García, K. Cruces, G. Ciudad, G. Chinga-Carrasco, Y. Habibi, ACS Sustain. Chem. Eng. 6 (2018) 12603–12612.
[26] G. Chen, T. Ushida, T. Tateishi, Macromol. Biosci. 2 (2002) 67–77.
[27] E.P. Barrett, L.G. Joyner, P.P. Halenda, J. Am. Chem. Soc. 73 (1951) 373–380.
[28] C.T. Molina, C. Bouallou, Clean Techn. Environ. Policy 18 (2016) 2133–2146.
[29] R. Zhang, C. Liu, P.C. Hsu, C. Zhang, N. Liu, J. Zhang, H.R. Lee, Y. Lu, Y. Qiu, Y. Cui, Nano Lett. 16 (2016) 3642–3649.
[30] E. Robles, I. Urruzola, J. Labidi, L. Serrano, Ind. Crop. Prod. 71 (2015) 44–53.
[31] M.E. Selamat, O. Sulaiman, R. Hashim, S. Hiziroglu, W.N.A.W. Nadhari, N.S. Sulaiman, M.Z. Razali, Measurement 53 (2014) 251–259.
[32] R. Mincheva, L. Jasmani, T. Josse, Y. Paint, J.M. Raquez, P. Gerbaux, S. Eyley, W. Wim Thielemans, P. Dubois, Biomacromolecules 17 (9) (2016) 3048–3059.
[33] D.O. Castro, J. Bras, A. Gandini, N. Belgacem, Carbohydr. Polym. 137 (2016) 1–8.
[34] H.M. Ng, L.T. Sin, T.T. Tee, S.T. Bee, D. Hui, C.Y. Low, A.R. Rahmat, Compos. Part B Eng. 15 (2015) 176–200.
[35] F. Rafieian, M. Hosseini, M. Jonoobi, Q. Yu, Cellulose 25 (8) (2018) 4695–4710.
[36] S. Sepahvand, M. Jonoobi, A. Ashori, F. Gauvin, H.J.H. Brouwers, Q. Yu, Polym. Compos. 41 (2020) 219–226.
[37] J. Feng, S.T. Nguyen, Z. Fan, H.M. Duong, Chem. Eng. J. 270 (2015) 168–175.